Clusterization-triggered emission: Uncommon luminescence from common materials

Haoke Zhang[1,2,#], Zheng Zhao[1,2,#], Paul R. McGonigal[3], Ruquan Ye[4], Shunjie Liu[1,2], Jacky W. Y. Lam[1,2], Ryan T. K. Kwok[1,2], Wang Zhang Yuan[5], Jianping Xie[6], Andrey L. Rogach[7], Ben Zhong Tang[1,2,8,*]

[1]Department of Chemistry, Hong Kong Branch of Chinese National Engineering Research Center for Tissue Restoration and Reconstruction and Institute for Advanced Study, The Hong Kong University of Science and Technology, Clear Water Bay, Kowloon, Hong Kong, China

[2]HKUST-Shenzhen Research Institute, No. 9 Yuexing 1st Rd, South Area, Hi-tech Park, Nanshan, Shenzhen 518057, China

[3]Department of Chemistry, Durham University, Lower Mountjoy, Stockton Road, Durham DH1 3LE, United Kingdom

[4]Department of Chemistry, State Key Laboratory of Marine Pollution, City University of Hong Kong, Kowloon 99077, Hong Kong, China

[5]School of Chemistry and Chemical Engineering, Shanghai Jiao Tong University, Shanghai 200240, China

[6]Department of Chemical and Biomolecular Engineering, National University of Singapore, 4 Engineering Drive 4, Singapore117585, Singapore

[7]Department of Materials Science and Engineering, and Center for Functional Photonics (CFP), City University of Hong Kong, 83 Tat Chee Avenue, Kowloon, Hong Kong, China

[8]Center for Aggregation-Induced Emission, State Key Laboratory of Luminescent Materials and Devices, SCUT-HKUST Joint Research Institute, South China University of Technology, Tianhe Qu, Guangzhou 510640, China

*Corresponding author at: Department of Chemistry, The Hong Kong University of Science and Technology, Clear Water Bay, Kowloon, Hong Kong, China. E-mail address: Tang, B. Z. (tangbenz@ust.hk).

[#]Zhang, H. and Zhao, Z. contributed equally to this work.

Keywords: Clusteroluminogens, Clusterization-triggered emission, Aggregation-induced emission, Through-space conjugation

Abstract

π-Conjugated chromophores have been investigated for many years and successful theoretical models have been developed to explain their photophysical properties. However, materials have appeared sporadically that do not fit within these existing models. Some of these materials possess entirely nonconjugated structures based on saturated C-C, C-O or C-N bonds, but their aggregates or solid-state forms show bright visible emission. This phenomenon is termed as clusterization-triggered emission (CTE) and the materials possessing the property are labeled clusteroluminogens. In this review, we provide a brief summary of the recent development of clusteroluminogens. The materials are classified into three categories: polymers (natural and synthetic polymers), small molecules (with and without aromatic rings) and metal clusters. Possible luminescence mechanisms underpinning the different categories of clusteroluminogens are analyzed individually. Finally, we put forward a comprehensive theory of the through-space conjugation (TSC) for these chromophores. Based on the CTE effect and TSC theory, various applications have been envisioned, for example in the areas of process monitoring, structural visualization, sensors, and probes. It is anticipated that this new research direction will bring many breakthroughs, not only in the theoretical areas, but also in these advanced applications of light-emitting materials.

1. Introduction

Throughout history, light has played a crucial role in the progression of human civilization. In today's society in particular, luminescence phenomena contribute greatly to our modern technologies and ways of life. There is continuous interest, therefore, in developing new luminescent materials with improved properties. Traditionally, ideal target molecules are considered to be organic dyes with fused aromatic rings, because of their high emission efficiencies, low weights, and high flexibilities[1-4]. Emission colors spanning from ultraviolet to near-infrared wavelengths can be accessed by tuning the length of their conjugated π-electron systems.[5-8] However, there are some drawbacks inherent to these materials. Firstly, extended conjugation is often accompanied with greater structural complexity, making some π-extended chromophores troublesome and expensive to synthesize. Secondly, synthetic processes can generate large amounts of waste, which is detrimental to the environment. Lastly, large benzannulated structures are often toxic to humans and can be resistant to degradation in the environment[9].

In addition, the planar conformations of traditional dyes are inherently linked to their conjugated electronic structures, allowing for better orbital overlap than twisted structures. While these planar structures often exhibit strong emission intensity in their 'single-molecule states'[10,11], e.g., when dissolved, the luminescence becomes weaker or is quenched entirely in aggregated states. This property of many π-conjugated chromophores is problematic, as it prevents their use as materials for solid-state devices[12]. This phenomenon, known as aggregation-caused quenching (ACQ), has been documented for more than half a century since Förster's discovery of concentration quenching effects in 1954[13].

In 2001, Tang et al. reported on a phenomenon that is antithetic to ACQ. They discovered that pentaphenylsilole is virtually nonluminescent in solution, but is highly emissive in aggregated states[14]. The term 'aggregation-induced emission' (AIE) was coined for this phenomenon[15], to contrast with the ACQ effects observed for traditional luminogens. A subsequent two decades of developments have revealed that AIE luminogens (AIEgens) possess many advantages over ACQ dyes[16-22]. Unlike traditional planar chromophores, the majority of AIEgens possess nonplanar structures and their intramolecular motions are hindered by steric overcrowding. Their highly emissive AIEgen films are among the best candidates for light-emitting materials and devices[23]. Meanwhile, the luminescence and hydrophilicity of AIEgens can be easily tuned by structural modification[24]. AIEgens are also of considerable interest for biological applications[25] as the physiological environment of bioassays is predominantly made up of aqueous media, in which hydrophobic aromatic compounds form aggregates or particles[26]. Consequently, traditional dyes that suffer from ACQ must be used at extremely low concentration in bio-imaging experiments as their high concentration would result in aggregation and quenching of the luminescence. In addition, a washing process is required after cell imaging to remove the interference caused by unlabeled ACQ dyes. These limits are easily overcome by utilizing AIEgens in place of traditional planar chromophores[27,28]. The imaging signal can be enhanced by increasing the amount of AIE probes. At the same time, the use of AIEgens endows the bio-imaging experiments with wash-free characteristics on account of the nonluminescent behavior of single-molecule species. AIEgens also have other favorable characteristics such as high photostabilities and large Stokes shifts (the difference between maximum absorption and emission wavelength), which had led to them being widely used in life sciences, optical electronics, and as chemoprobes or bioprobes, etc[29-36].

Although AIEgens overcome many of the drawbacks associated with traditional, planar chromophores, their use in bioassays is restricted by their cytotoxicity[37,38]. In principle, nonaromatic systems are attractive candidates to overcome this issue, some of the most abundant, non-toxic natural products, such as starch, cellulose, and proteins, are either entirely nonaromatic [39,40] or include only small, isolated aromatic systems with only short-range electron delocalization[41-43]. Additionally, compared with synthetic aromatic systems, natural products offer other potential advantages. They are abundant in nature, so they are generally accessible at low cost, and their biocompatibility is better than the artificial materials, which makes them environmentally friendly. Indeed, the mechanoluminescence of sugar was documented in the book of "Advancement of Learning" in 1605 by Sir Francis Bacon[44]. Recently, several research groups have reported the luminescent behaviors of proteins, starch, sodium alginate (SA), etc.[45-49] However, it has been a challenge for physicists and chemists to draw a clear mechanistic picture that explains why these simple and nonconjugated structures emit visible light. Progress has been slowed by the perception that instances of nonconventional luminescence can be ascribed solely to low levels of luminescent contaminants, which, although likely responsible in a few isolated cases, is now an unsatisfactory explanation to account for a wealth of experimental data on the topic. The lack of a clear working mechanism for these materials has been a bottleneck that has hindered their further development and application.

Learning from nature, is it possible to design AIEgens with nonconjugated structures and highly efficient photophysical performances? In 2007, some of us reported on colloidal suspensions of the nonaromatic poly[(maleic anhydride)-*alt*-(vinyl acetate)] (PMV) emit blue light under UV irradiation while its diluted solution was nonluminescent, exhibiting properties comparable to AIEgens[50,51]. Similar effects have been observed prior to or since 2007 for siloxanes[52-57], poly(amidoamine) (PAMAM)[58-61] and polypeptides[62-64]. We have denoted this process as *clusterization-triggered emission* (CTE)[51,65-67]. The emission is described as clusteroluminescence and the chromophores responsible for it are classified as *clusteroluminogens*[68]. More recently, Tomalia, Klajnert-Maculewicz et al. have described the phenomenon using the term 'non-traditional intrinsic luminescence' (NTIL)[69-72]. In essence, the photophysical characteristics of NTIL are similar to CTE. By summarizing all the CTE-related studies, several common features have been identified for clusteroluminogens: (i) their chemical structures are apparently nonconjugated and functional groups with nonbonding or π-electrons are separated by a saturated σ-bonded backbone[73,74]; (ii) in isolation, i.e., when they are dissolved at low concentrations, they are nonluminescent, but clusteroluminescence is observed in clustered states[51]; (iii) their absorption and excitation spectra are quite different from one another, the longest-wavelength peaks of their excitation spectra are generally not detectable as a significant feature in absorption spectra [75]; (iv) the wavelength and intensity of their emissions are size- or generation-dependent for particles and dendrimers, respectively [76-78]; (v) their emission intensities and wavelengths are size-dependent for the nanoparticles, or generation-dependent for dendrimers[79,80]; (vi) some clusteroluminogens are capable of phosphorescence, including room-temperature phosphorescence (RTP)[81,82]. Taken together, these characteristics of clusteroluminogens make them appealing targets for further investigation and multifunctional applications.

In this review, the luminescence of clusteroluminogens will be reevaluated and viewed through the lens of CTE. In section 2, clusteroluminogens will be classified into three categories: polymers, small molecules and metal clusters. We subdivide discussion of polymers into natural and synthetic polymers and deal separately with small molecules that either contain some small aromatic groups or that are fully non-aromatic. We note that aromatic clusteroluminogens still

have nonconjugated structures in which the π units are separated by saturated alkanes[83]. In section 3, several reported hypotheses on the emission mechanism of clusteroluminogens are summarized, and based on them, we propose mechanistic picture of the through-space conjugation (TSC) for CTE, which we hope will serve as a foundation for others to understand and expand upon the photophysical process underpinning clusteroluminescence. Finally, in Section 4, we introduce a selection of some applications of clusteroluminogens, such as monitoring and visualization of biological/abiologic process and structures, sensors and probes. Clusteroluminogens have potential for valuable applications in biology in particular on account of their good biocompatibilities. We hope that this review will offer comprehensive treatment of this phenomenon, and eventually lead to a surge in applications of clusteroluminogens.

2. Structural diversity of clusteroluminogens

As mentioned above, the mechanoluminescence of sugar was discovered by Sir Francis Bacon as far back as in 1605 when scratching sugar with a knife[44]. Systematic investigations into this type of non-traditional luminescence were started around 2000 by Tucker, Goodson, Tomalia and Tang et al[58,59], including demonstration of intrinsic emission from nonconjugated PAMAM and PMV, which are nonconjugated polymers. Meanwhile, with an evolving CTE concept, it has become clear that mechanism of clusteroluminescence is rather different from the traditional photophysical theories that apply to π-conjugated systems. In the forthcoming part, we examine the structures of clusteroluminogens by dividing them into three categories: polymers, small molecules, and metal clusters.

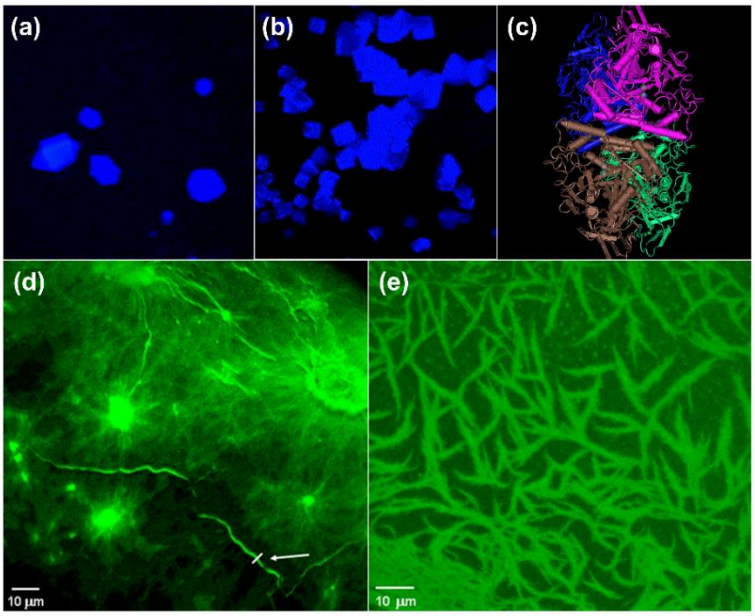

Figure. 1 Photographs of (a) Hydantoinase and (b) truncated (βαβ) Pyrococcus furiosus protein taken under 364 nm UV light. Reprinted with permission from ref 89. Copyright 2004 Elsevier Inc. (c) Structure of D-hydantoinase. Ref 90. Copyright 2003, American Society for Microbiology. Confocal microscopy images of the poly(ValGlyGlyLeuGly) amyloid-like fibrils at concentrations of (d) 1.0 mg/mL and (e) 0.1 mg/mL. Ref 92. Copyright 2007, National Academy of Sciences.

2.1 Polymers

2.1.1 Natural polymers

In the 1960s, green fluorescent protein (GFP) was purified from Aequorea victoria and its optical and structural properties were studied by Shimomura, who was awarded the Nobel Prize in Chemistry in 2008 for the discovery and development of GFP together with Chalfie and Tsien[84,85]. Investigations into the chemical structure of GFP have revealed that its green emission stems from its 4-(*p*-hydroxybenzylidene)imidazolidin-5-one chromophores[86,87]. However, there are other examples of enzymes and proteins that are known to emit visible light, but lack identified chromophores[88]. For example, in 2004, Guptasarma et al. observed blue emission from hydantoinase and truncated (βαβ) pyrococcus furiosus protein (Fig. 1a&b)[89]. Fig. 1c shows the crystal structure of D-hydantoinase[90]. They proposed that the intrinsic fluorescence did not originate from any aromatic residues, and that formation of hydrogen bonds between C=O and N-H groups of these species caused the inter- or intramolecular electron delocalization[91]. Rinaldi et al. observed the green emission from poly(ValGlyGlyLeuGly) amyloid-like fibrils in 2007(Fig. 1d&e)[92]. They found that the emission intensity was strongly dependent on the retention of water molecules, which suggested that the water molecules bound to the proteins played an important role in the emission mechanism.

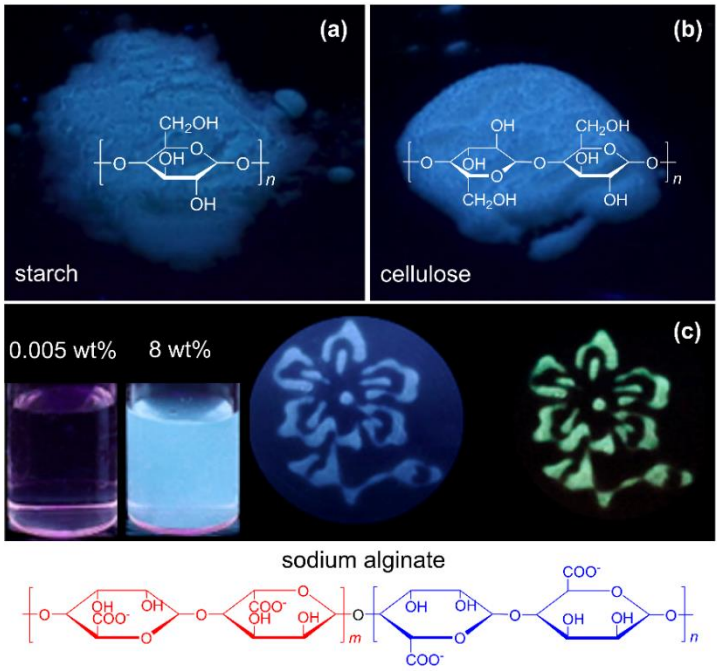

Figure. 2 Photographs of solid powders of (a) starch and (b) cellulose taken under 365 nm irradiation at room temperature. Reprinted with permission from ref 39. Copyright 2013, Science China Press and Springer-Verlag Berlin Heidelberg. (c) Left: photographs of aqueous solutions of SA (0.005 and 8 wt%, respectively) taken under 365 nm irradiation; Right: Photographs of a flower drawn on a polytetrafluoroethylene plate using 8 wt % SA aqueous solution, taken under 312 nm irradiation (blue pattern) and after UV irradiation was removed (yellow-green pattern). Reprinted with permission from ref 93. Copyright 2018, American Chemical Society.

Beyond proteins, other biopolymers such as starch, cellulose and SA exhibit clusteroluminescence. As shown in Fig. 2, faint blue emission can be observed for these three

polysaccharides[39]. It is noteworthy that visible emission is only observed in aggregated or solid states but not in their diluted solutions. Additionally, RTP was detected in these natural polymers. Fig. 2c shows that the SA film emits blue fluorescence under 312 nm UV irradiation[93]. While yellow-green phosphorescence appeared once the UV light was removed. Noteworthy, the RTP comes from the amorphous state but not crystalline one. Pure organic RTP in the crystalline state is well-studied but examples involving amorphous solids are rare, providing further motivation to investigate the mechanistic role of this clusteroluminescence in RTP.

2.1.2 Synthetic polymers

The same problem has also held back the study of poly(amidoamine) (PAMAM) dendrimers, whose structures include amido, amine and alkyl groups (Fig. 3a)[94-96]. The first starburst-dendritic PAMAM was synthesized by Tomalia et al. in 1985[97]. The nonconjugated structure of PAMAM, which lacks a traditional fluorescent chromophore, would suggest that it should be nonluminescent. However, its weak emission has been observed many times since it was first synthesized. For example, in 1990, Tomalia et al. used a fluorescence method to investigate anionic PAMAM dendrimers with pyrene as a probe[98]. At that time, they stated that: "*Pyrene lifetime measurements were attempted, but the experiments were viciated by the presence of a contribution to the decay due to the starburst dendrimers. Starburst emission intensity in the steady-state measurements was always negligible*". Ten years later, Tucker explicitly pointed out the presence of intrinsic fluorescence from PAMAM[58]. Detailed photophysical studies indicated that the weak, but detectable, fluorescence was most likely due to the n–π^* transition from the amido groups. Other dendrimers with intrinsic fluorescence were also described, such as dendrimers based on poly(α-amino acid) and poly(propylene imine) (PPI)[62,99-103]. It is noteworthy that, in contrast to PAMAM, PPI has no π electrons as part of its structures, but only n electrons.

These discoveries naturally led to the role of the polymer architecture being examined. Liu et al. designed hyperbranched poly(amino ester)s with varying terminal groups (Fig. 3b)[104]. In terms of their structural units, poly(amino ester)s and PAMAM are similar to one another, and for the later it was proposed that the intrinsic fluorescence was induced by the oxidation of amine[105]. In Liu's work, all the experiments were performed under an argon atmosphere, including the polymerization, purification and fluorescence measurements, but even then, fluorescence was observed for all the hyperbranched polymers. They thus concluded that fluorescence was an inherent property of these dendritic or hyperbranched polymers rather than being caused by oxidation. This hypothesis has been supported further by observation of fluorescent emission from hyperbranched polyethylenimine (PEI), showing that dendritic architectures are not unique in creating fluorescent species[106]. Indeed, Stiriba et al. subsequently demonstrated that a high degree of polymer branching, in general, is not a prerequisite for this type of luminescence. They reported that linear PEI derivatives are more emissive than hyperbranched ones (Fig. 3c). Consequently, research into the CTE of synthetic polymers has since shifted from varying polymer architectures to investigating different chemical structures[107-109]. In addition to the nitrogen-based polymers discussed above, other structures based on other heteroatoms, such as poly(ethylene glycol) (PEG)[110] and polydimethylsiloxane (PDMS)[111] were also reported to have intrinsic fluorescence.

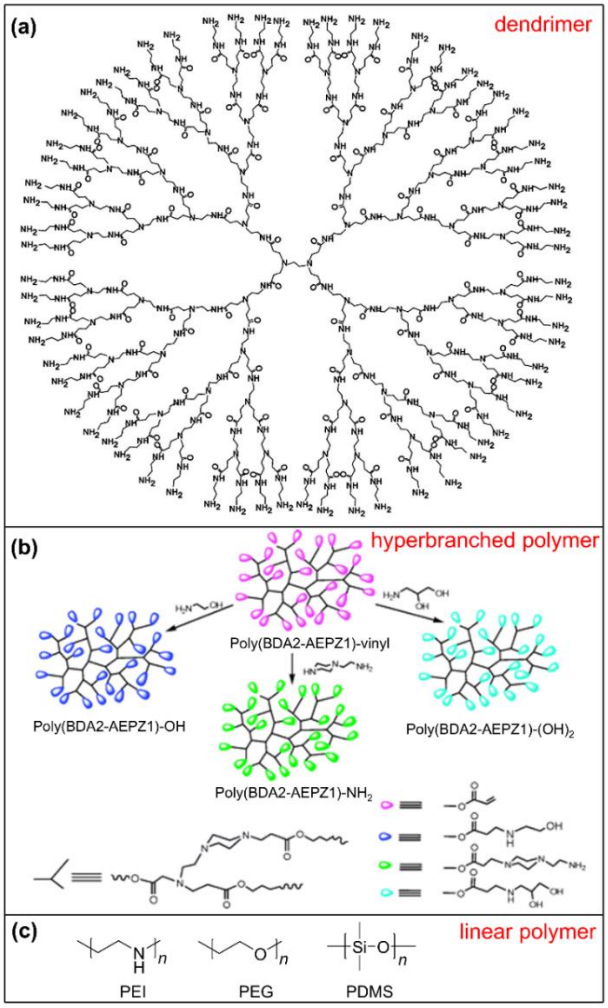

Figure. 3 Structures of (a) a PAMAM dendrimer. Reprinted with permission from ref 94. Copyright 2015 Elsevier Inc. (b) Poly(amino ester)s hyperbranched polymer. Reprinted with permission from ref 104. Copyright 2005, American Chemical Society. (c) Polyethylenimines (PEI), poly(ethyleneglycol) (PEG) and polydimethylsiloxane (PDMS) linear polymers.

PMV is a well-studied copolymer that can be prepared as microspheres with uniform sizes, reactive surfaces, and desirable solubilities[112-114]. In 2007, some of us observed blue intrinsic fluorescence from PMV under 365 nm irradiation (Fig. 4a)[50]. Meanwhile, we observed that its emission intensity is enhanced with increasing concentration. Wang et al. replaced the vinyl acetate monomer with vinyl pyrrolidone to synthesize poly[(maleic anhydride)-*alt*-(vinyl pyrrolidone)] (PMVP) copolymers[75]. The polymerization was performed with monomer concentrations of either 2 M or 10 M, producing the copolymers PMVP-2 and PMVP-10, respectively. PMVP-10 had a lower molecular weight (M_w) than PMVP-2, but unlike PMVP-2 which had a sky-blue emission, PMVP-10 emitted yellow fluorescence in the powder (Fig. 4b). The authors attributed this phenomenon to the strong entanglement of the longer PMVP-2 polymers chains, which inhibited the aggregation of anhydride and pyrrolidone groups, and impeded the formation of large-sized clusters. In addition, the red-shifted emission of PMVP as compared to PMV was ascribed to the introduction of pyrrolidone groups reducing the rigidity of polymer chains, thus increasing the interactions between the anhydride and pyrrolidone groups. Comparison of

PMV and PMVP shows a vinyl acetate group is not necessary for clusteroluminescence. Indeed, Pucci et al. synthesized polyisobutene succinic anhydride (PIBSA), where succinic anhydride made up the terminal groups[115]. Unexpectedly, the PIBSA still emitted light at around 400 nm, though its intensity was weak. Condensation reaction of PIBSA with triethylenetetramine (TETA) generated crosslinked polyisobutene succinimides (PIBSI bis), whose emission intensity was much stronger than that of the reactants (Fig. 4c). This effect was used to monitor the reaction progress, which will be discussed further in Section 4. In order to further investigate the role of succinic anhydride in the clusteroluminescence, Qiao et al. carried out the hydrolysis of PMV in a strongly alkaline solution of sodium hydroxide[116-118]. The hydrolysis product PMV-Na showed strong and sky-blue emission as powder, and even brighter red emission appeared when the PMV-Na was thermally treated under 180 °C for 5 min (Fig. 4d). Thus, the emission color of PMV derivatives covers the broad range of emission wavelength, from deep blue to red.

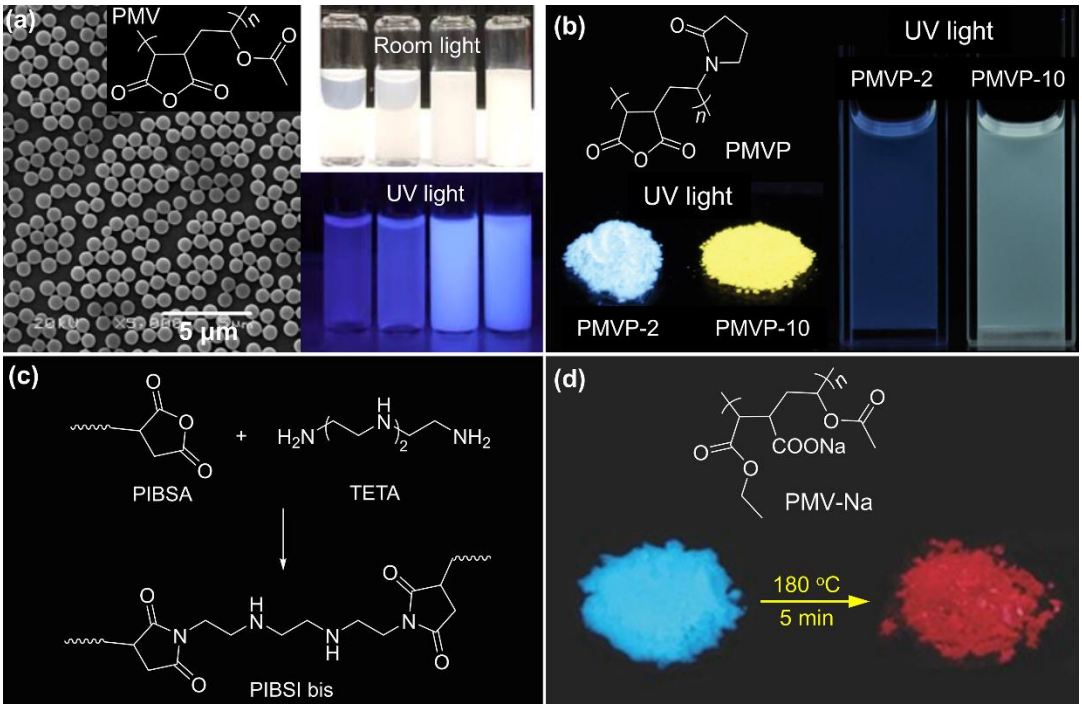

Figure. 4 (a) SEM microphotograph of colloidal PMV particles and photographs of PMV solution with different concentration suspensions taken under room light (top) and 365 nm irradiation (bottom). Concentrations: from left to right, 0.05, 0.1, 1, and 10 wt%. Ref 50. Copyright 2007 American Chemical Society PMSE Division. (b) Photographs of two PMVP copolymers as powder and DMSO solutions (10^{-3} g/mL) taken under 365 nm irradiation. PMVP-2 and PMVP-10 stay for copolymerization with different monomer concentration; see text for details, Reprinted with permission from ref 75. Copyright 2017 Royal Society of Chemistry. (c) The condensation reaction of PIBSA with TETA. Ref 115. (d) Photographs of PMV-Na powders (hydrolysis products of PMV) before (left) and after thermal treatment (right) taken under 365 nm irradiation. Reprinted with permission from ref 116. Copyright 2017 WILEY‐VCH Verlag GmbH & Co. KGaA, Weinheim.

2.2 Small molecules

As mentioned above, the intrinsic luminescence of some natural polymers had been observed for a long time without attracting much attention because of difficulties in fully elucidating their structures and the key functional groups. Although the subsequently studied synthetic polymers have well-defined repeat units, the presence of impurities is difficult to rule out entirely, particularly given the heterogeneous nature of polymers and limitations in their purification. Unambiguous interpretations drawn from the photophysical studies require both an explicit chemical structure and high purity of the materials[119-125]. To overcome this issue, researchers turned the focus of the studies towards small-molecule materials, which can satisfy the aforementioned two requirements. In this section, we will focus on two sorts of small molecules: clusteroluminogens with and without aromatic rings.

2.2.1 Clusteroluminogens containing aromatic rings

In 1963, Lumry et al published a research article entitled '*Fluorescence of Styrene Homopolymers and Copolymers*[126]', where red-shifted emission in isotactic polystyrene (PS) compared to the atactic one has been reported. Atactic PS showed almost the same absorption and emission spectra as benzene[74,127]. Meanwhile, poly(styrene-*co*-methyl methacrylate) showed similar maximum emission wavelength ($\lambda_{max\text{-}em}$) to atactic PS and the $\lambda_{max\text{-}em}$ decreased with the decrease of styrene fraction. All these results suggested that intra-/intermolecular interactions among neighboring isolated phenyl rings played an important role for the red-shifted emission. However, this work has largely been overlooked in contemporary literature, perhaps because of the unclear mechanistic picture of the abnormal fluorescence in isotactic PS. Half a century later, Tang et al. reproduced this phenomenon in 1,1,2,2-tetraphenylethane (*s*-TPE), which lacks through-bond conjugation among its four aromatic rings (Fig. 5a)[74,128-130]. Tetrahydrofuran (THF) solutions of *s*-TPE exhibit a 290 nm emission peak, which was assigned to the isolated phenyl rings' electronic transitions. Addition of water firstly increased the phenyl emission, which was attributed to the increasing solvent polarity. At a fractional water content, f_w, of 70%, a new peak appeared around 460 nm along with a decrease of the 290 nm emission intensity. Further increasing the f_w made the longer-wavelength emission become stronger and stronger. It has been proved that aggregates of *s*-TPE were formed at $f_w \geq 70\%$. The inset in Fig. 5a shows the bright cyan emission of *s*-TPE powder. The 460 nm emission from *s*-TPE could be ascribed to typical CTE. X-ray crystallographic analysis of crystalline *s*-TPE and the related theoretical calculations revealed the existence of through-space conjugation among four benzene rings in *s*-TPE[130-132], whose detailed mechanistic picture will be further explained in Section 3.

Other phenyl-containing clusteroluminogens[133], such as compound **1** and tetrathienylethene (TTE), were also reported to possess red-shifted emissions in their aggregated states. As shown in Fig. 5b, the two aromatic rings of **1** are separated by a central four-membered ring with a sp^3-C that interrupts conjugation between the aromatic groups[134]. The PL spectrum of **1** in THF showed only the isolated aromatic rings emission around 300 nm, consistent with its electronically nonconjugated structure. However, a new peak at 400 nm appears in the aggregated state at f_w = 80%, and its solid-state PL spectrum reveals only 400 nm emission with the complete disappearance of the 300 nm peak. The authors concluded that the longer-wavelength emission originated from intramolecular TSC. The same phenomenon was also reported for TTE. Its solution-state emission is dominated by through-bond conjugation among the peripheral thiophenes and the central double bonds (Fig. 5c)[135]. On the contrary, visible blue emission is observed from TTE aggregates and powders as a consequence of inter-/intramolecular S···S

interaction[136,137]. In addition to TTE, the well-studied AIEgen tetraphenylethylene (TPE) also shows the unexpected emission at 470 nm. Recently, Tang et al. proved that the 470 nm emission in TPE arises from the intramolecular TSC among four phenyl rings rather than through-bond conjugation. The emission is similar to that from *s*-TPE, they give comparable PL spectra in the solid state[138]. Meanwhile, previously reported solution-state PL spectra of TPE have always exhibited a weak peak around 400 nm, which has previously been mistakenly ascribed to an impurity[139,140], but can now be attributed to TSC. Tang et al. also confirmed that the through-bond conjugation of a "photocyclized" intermediate induced this shorter-wavelength emission[141,142]. Based on these considerations, we classify the above-mentioned small molecules as clusteroluminogens.

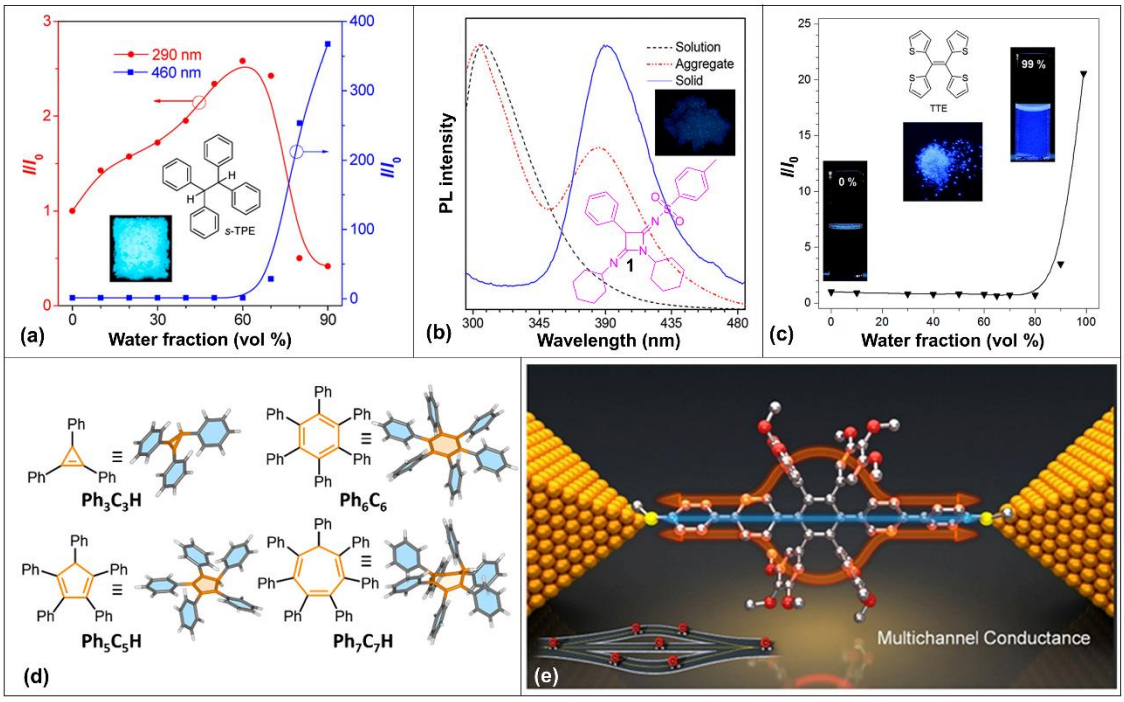

Figure. 5 (a) Plots of I/I_0 versus the f_w for THF/water mixture of *s*-TPE. Two emission wavelengths are monitored: 290 nm (red line) and 460 nm (blue line). *I*: fluorescence intensity, I_0: fluorescence intensity at f_w = 0%. Inset: photograph of the powder of *s*-TPE taken under 365 nm irradiation. (b) PL spectra of compound **1** in different states. Inset: photograph of the powder of **1** taken under 365 nm UV irradiation. (c) Plot of I/I_0 at 410 nm versus the f_w for THF/water mixtures of TTE. Inset: photographs of the TTE taken under 365 nm irradiation, from left to right: a THF solution, a powder and an aggregated suspension with f_w = 99%. Ref 135. Copyright 2017 Royal Society of Chemistry. (d) Structural formulae and X-ray crystal structures of Ph_3C_3H, Ph_5C_5H, Ph_6C_6, and Ph_7C_7H. Ref 74, ref 134 and ref 143. Copyright 2017 American Chemical Society. (e) Schematic representation of a multichannel conductance in Ph_6C_6 derivative. Ref 144. Copyright 2018 American Chemical Society;

McGonigal et al. have reported the observation of excited-state aromatic interactions in phenyl-ring molecular rotors (Fig. 5d)[143]. They examined steady-state PL spectra and employed theoretical calculations to study TSC in Ph_3C_3H, Ph_5C_5H, Ph_6C_6, and Ph_7C_7H. A significant influence of TSC on emission energy from the phenyl-ring rotors was only observed for Ph_5C_5H and Ph_7C_7H. The overcrowding of phenyl rings in Ph_7C_7H promotes formation of an excited-state through-space aromatic dimer (ESTSAD) involving the isolated phenyl ring bonded to an sp^3-C

center. A weaker effect was observed for the less crowded Ph_5C_5H compound. Although there is an isolated phenyl ring in the structure of Ph_3C_3H, the longer distance between neighboring phenyl rings limited the formation of an ESTSAD. Moreover, the rigid core of Ph_6C_6 hindered the excited-state molecular motion. So, from the point of view of photoluminescence, there is no observation effect of TSC in Ph_6C_6. However, recently, Zhao et al. reported the multichannel conductance of single-molecule wires consisting of Ph_6C_6 derivatives, which proved the existence of TSC in these molecules' charge transport[144,145]. With the caveat that these two reports deal with different compounds under different conditions, it is intriguing that the TSC in such similar structures apparently influences electron delocalization in photoexcited states and charge transport differently. Further investigation is required to gain a deeper understanding of the factors causing this apparent difference.

2.2.2 Clusteroluminogens without aromatic rings

Poly(amino acids) have been reported to show clusteroluminescence in the aggregated state[73]. Preliminary results indicated that through-space electronic communication by O···O, N···N, N···C=O, O···C=O and C=O···C=O short contacts may contribute to the clusteroluminescence. Theoretically, therefore, pure amino acids could also be emissive as analogous interactions can arise in their aggregated states, notwithstanding that polymer entanglement might enhance the inter-/intra-chain interaction and lead to an increase of the emission intensity. Indeed, Yuan et al. have observed bright emission from recrystallized amino acids(Fig. 6)[146]. Notably, *L*-isoleucine fluoresces a yellow-green color under 365 nm irradiation and the luminescence quantum yield (Φ_L) of *L*-lysine is as high as 7.4%. Most of these materials also exhibit low-temperature phosphorescence.

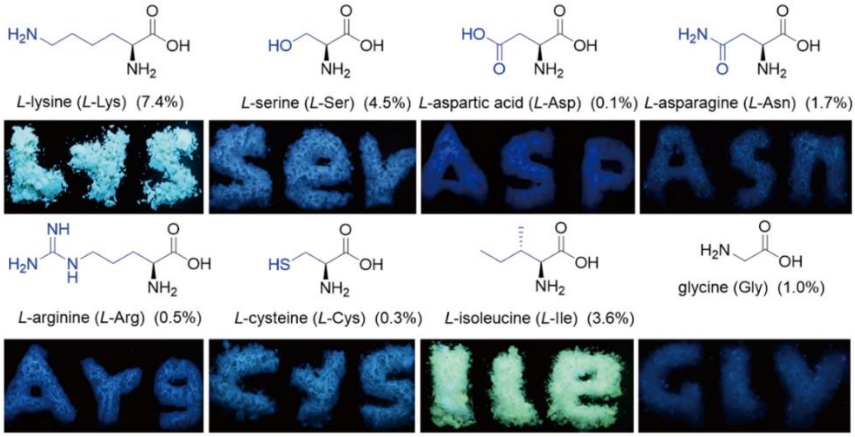

Figure. 6 Photographs of recrystallized amino acids taken under 365 nm irradiation. Structural formulae are provided on top of each image, number in brackets indicate solid-state luminescence quantum yields. Reprinted with permission from ref 146. Copyright 2017, Science China Press and Springer-Verlag GmbH Germany.

Simple functional groups such as C=O, C-O, C-N, etc. are present in different amino acids whose intrinsic luminescence apparently originated from inter-/intramolecular TSC. It is worth considering, therefore, that many common N, O, S, P, etc. heteroatom-based nonconjugated small molecules may also exhibit clusteroluminescence. For example, as shown in Fig. 7a, compound **2** is a simple aliphatic oxime in which the C=N-O group is the only through-bond conjugated unit[147]. However, a bright blue emission with $\lambda_{max\text{-}em}$ = 450 nm was detected from an

ethanol solution of **2** and the emission intensity was enhanced by increasing its concentration. Meanwhile, the excitation spectra were almost symmetrical to the PL spectra. Compounds **3** and **4** also exhibit CTE[148]. Compound **3** gives rise to a redder and stronger clusteroluminescence than **4**, which is presumably a result of the additional double bond extending through-bond conjugation. In each of **2**-**4**, there is some form of double bond, i.e., C=C, C=O or C=N groups, which may play an important role in the CTE effect. This begs the question, is clusteroluminescence possible in a pure *n*-electron system? Indeed, as we mentioned in Section 2.1.1, PPI, PEI, PEG and PDMS are all clusteroluminogens possessing *n* electrons and no π electrons. Accordingly, we might expect that certain *n* electron-based small molecules may also show CTE.

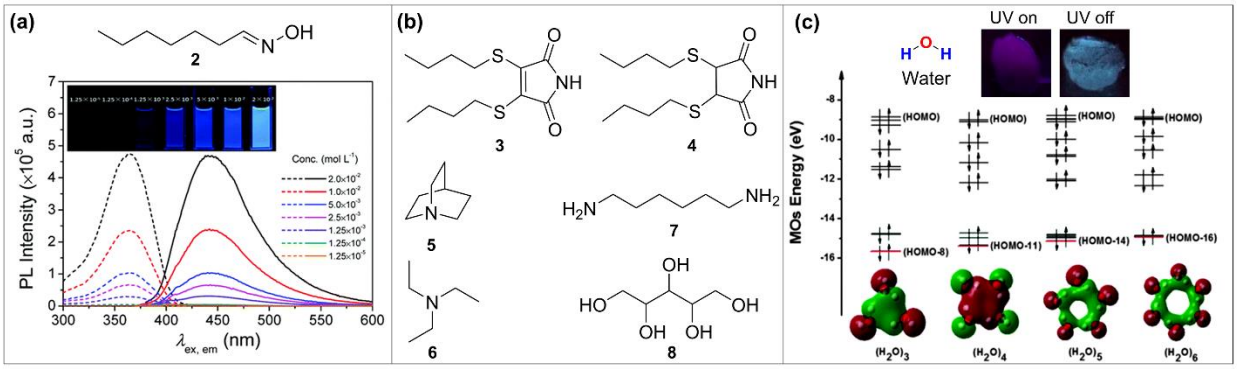

Figure. 7 (a) Fluorescence excitation (dashed lines) and emission spectra (solid lines) of compound **2** in ethanol with different concentrations. Inset: respective photographs taken under 365 nm irradiation. Reprinted with permission from ref 147. Copyright 2017, Royal Society of Chemistry. (b) Chemical structures of compounds **3–8**. (c) Upper row: Photographs of frozen water at 77 K taken under 312 nm irradiation and immediately after stopping UV irradiation. Bottom: Energy level diagrams of various small water clusters. The red lines correspond to the energy levels of the characteristic occupied molecular orbital presented in the bottom diagram. HOMO: Highest occupied molecular orbital. Reprinted with permission from ref 158. Copyright 2015, Royal Society of Chemistry. Ref. 160, Copyright 2019, WILEY‐VCH Verlag GmbH & Co. KGaA, Weinheim

In 1970, Halpern et al. reported the unexpected fluorescence in tertiary amine derivative **5** in which a broad peak with $\lambda_{max\text{-}em}$ = 310 nm was observed at 250 nm excitation[149]. They attributed this intrinsic fluorescence to a weak *V* ← *N* state (where *N* is the ground state and *V* is the electronic state in which one electron for the *n* orbital has been excited to the *σ** orbital)[150-152]. In 2009, Imae et al. discovered the blue fluorescence in triethylamine (**6**) in the process of investigating PAMAM fluorescence[153]. In this work, they ascribed the blue emission to exciplex formation between O_2 and the tertiary amine. Recently, we also observed blue fluorescence in aliphatic primary amine **7**, which proved that the tertiary amine was not an indispensable part of clusteroluminescence[154]. Further studies excluded the interferences of impurities and oxidation. Hydrogen-bonding interactions of **7** were believed to induce the self-association and through-space electron communication responsible for its intrinsic blue emission. In addition to these nitrogen-based systems, oxygen-based pure *n* electron clusteroluminescence has also been detected in xylitol (**8**) whose $\lambda_{max\text{-}em}$ is located at 360 nm[110]. Additionally, xylitol exhibits RTP. Recently, Wang's group have summarized the electron density delocalization of hydrogen-bonded systems[91]. It is generally agreed that the hydrogen bonds involve not only an electrostatic interaction, but they also induce electron density delocalization[155-157]. As shown in Fig. 7c, first-

principles computer modeling of ring-shaped water clusters suggests that increasing cluster size leads to increased electron delocalization and a characteristic orbital shift in occupied orbitals[158]. In 1999, Lobyshev et al. reported the intrinsic luminescence of water and its PL spectra have been collected[159]. The $\lambda_{max\text{-}em}$ of water is 350 and 410 nm under the 260 and 310 nm excitation, respectively. Recently, Yuan et al. observed the afterglow emission when the water was frozen to 77K. Fig. 7c shows a cyan emission that is observed after switching off the UV lamp[160].

2.3 Metal clusters

We have introduced pure organic clusteroluminogens in the above two parts. In 2012, Xie et al. have reported the AIE effect of oligomeric Au(I)−thiolate complexes which were synthesized from $HAuCl_4$ and reduced L-Glutathione (GSH). GSH contains carboxylic, amine, amide and thiol groups[161]. The Au(I)−thiolate complexes show no emission in aqueous solution, but bright emission appears upon aggregation triggered by the addition of ethanol, with its color gradually changing from red to orange (Fig. 8a left). Apparently, the optical characteristics of the Au(I)−thiolate complexes are in analogy with the linear and dendritic polymers-based clusteroluminogens, which are classified as exhibiting CTE. Au(0)@Au(I)−thiolate nanoclusters (NCs) were obtained from the same reactants as the Au(I)−thiolate complexes, but using different reaction conditions. The resultant Au−thiolate NCs showed strong orange luminescence both in solution and solid states (Fig. 8a right), which suggests that they may already aggregate in solution. The authors tried to separate the Au−thiolate NCs by native polyacrylamide gel electrophoresis (PAGE). From band 1 to 5 (Fig. 8a), the molecular weight of the fractions increased; but contrary to the prediction from the Jellium model, where larger-sized NCs should emit at longer wavelengths, a blue-shifted $\lambda_{max\text{-}em}$ was found for species from 1 to 5. Recently, Konishi et al. identified fluorescence-to-phosphorescence switching process for the gold NCs, namely ($[Au_8(dppp)_4L_2]X_2$) [162]. These Au_8 clusters emitted with $\lambda_{max\text{-}em}$ = 600 nm in the solution state but phosphorescence at 700 nm was detected in the solid state, as is schematically shown in Fig. 8b. Other metals in the form of NCs, such as silver and copper have also shown aggregation-induced fluorescence enhancement phenomena[163-171], which has been used, for example, to fabricated down-conversion white light-emitting devices (WLED) [172]. As shown in Fig. 8c, orange emitting, aggregated-on-purpose Cu NCs were synthesized from Cu^{2+} and GSH, and blue-emitting ones from Cu^{2+} and polyvinylpyrrolidone (PVP). The combination of these orange and blue emitting Cu NC species has been used to produce WLEDs. Notably, both the GSH and PVP exhibit non-conjugated structures, and the complexation of these molecules with Cu metal core produced metal clusters with AIE, and eventually CTE effects.

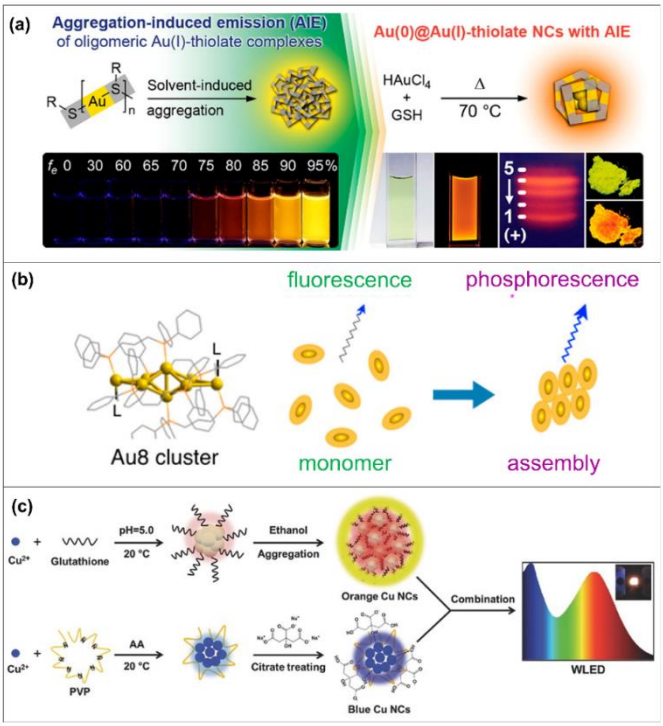

Figure. 8 (a) Left: AIE properties of oligomeric Au(I)−thiolate complexes in water/ethanol mixtures with the ethanol fraction (f_e) increasing from left to right. Right: the synthetic route towards Au(0)@Au(I)−thiolate nanoclusters (NCs), together with photographs of these NCs in water (in cuvettes) and in solid state taken under daylight and UV irradiation, and photograph of PAGE bands of the NCs taken under UV light. Ref 161. Copyright 2012, American Chemical Society. (b) Schematic illustration of the Au_8 NCs ($[Au_8(dppp)_4L_2]X_2$) which experience fluorescence in the monomeric form and phosphorescence in the aggregate states. Ref 162. Copyright 2017, American Chemical Society. (c) Schematics of the formation and treatment of orange and blue emitting Cu NCs, and their combination as phosphors in a down-conversion white light-emitting devices (WLED). Ref 172. Copyright 2016, WILEY-VCH Verlag GmbH & Co. KGaA, Weinheim.

3. Mechanistic studies of clusteroluminescence

In this section, we will briefly introduce recent progress in the mechanistic studies of clusteroluminescence. Clusteroluminogens with polymeric and monomeric structures are classified as organic species, and the metal clusters will be discussed individually. At the end of this section, we will draw a comprehensive mechanistic picture for the CTE process.

3.1 Organic clusteroluminogens

Some photophysical mechanisms have been mentioned in the preceding Section dealing with *Structural Diversity*. Before clarifying these mechanisms in detail, some typical features inherent the organic clusteroluminogens will be presented here, such as generation-, molecular weight- and excitation wavelength-dependent luminescent properties. As shown in Fig. 9a, fourth generation (G4) PAMAM dendrimers exhibit a red-shifted and enhanced emission relative to second generation analogs (G2)[173]. It is reported that the lower generation PAMAM dendrimers

have an “open” configuration but a crowded structure is found in high generation ones, supporting the idea that clusterization or rigidification of certain units in the structure plays an important role in the clusteroluminescence. The same effect is also reflected in trends observed by varying polymer molecular weight (M_n). With increasing M_n, the enhanced inter-/intra-chain entanglement interaction boosts rigidification and intrachain contacts. Fig. 9b shows that the PL spectra of PMVP in DMSO solution undergo a bathochromic shift from 440 to 540 nm upon the increasing of M_n[75]. Meanwhile, the fluorescence intensities are enhanced simultaneously. Most clusteroluminogens, if not all, exhibit excitation-dependent emission properties[174,175]. In 2015, Zhu et al. reported multicolor emission resulting from different wavelengths being used to excite linear and hyperbranched PAMAM (Fig. 9c)[176]. They hypothesized that the different emission profiles stemmed from different clustering species in these polymers. Recently, Tang et al. have concluded that most clusteroluminogens have red-shifted excitation spectra relative to absorption[41]. For example, Fig. 9d illustrates that PEG 3350 has extremely weak absorption above 300 nm. However, it fluoresces when excited in this region and the excitation spectrum peaks around 330 nm.

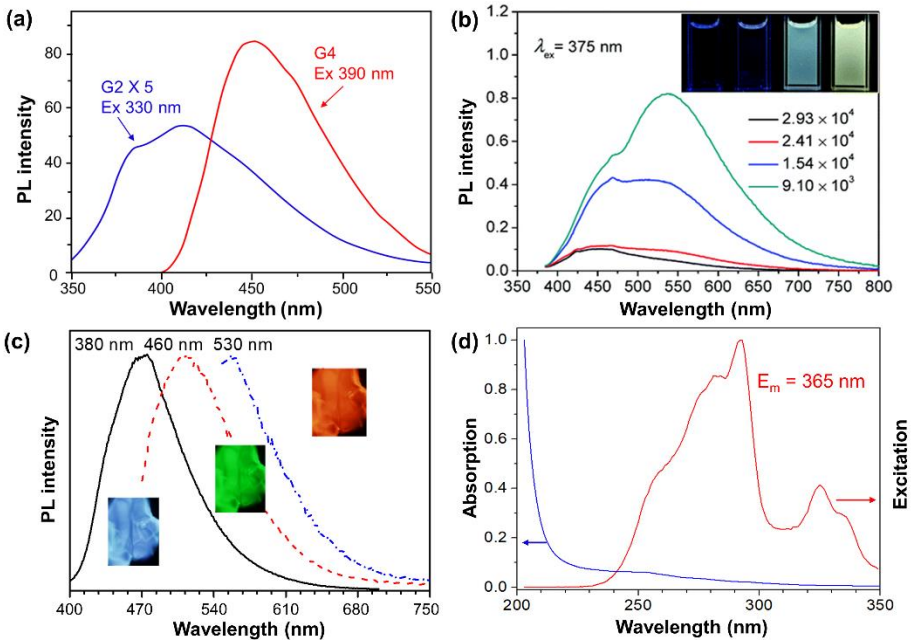

Figure. 9 (a) PL spectra of second (G2) and fourth (G4) generation NH_2-terminated PAMAM dendrimers at pH = 2 in aqueous solutions. Ref 173. Copyright 2004, American Chemical Society. (b) PL spectra of PMVP in DMSO solution with different molecular weight, as indicated on the frame; concentration = 10^{-3} g/mL. Labels show average M_n in g/mol. Reprinted with permission from ref 75. Copyright 2017 Royal Society of Chemistry. (c) PL spectra and the respective photographs of solid films casted from linear PAMAM, taken at different excitation wavelengths, as indicated on the frame. Reprinted with permission from ref 176. Copyright 2015, Chinese Chemical Society, Institute of Chemistry, Chinese Academy of Sciences and Springer-Verlag Berlin Heidelberg. (d) Absorption and excitation spectra of PEG 3350 in aqueous solution.

In order to explain these phenomena, Tang et al. synthesized oligo(maleic anhydride) (OMAh) and poly[(maleic anhydride)-*alt*-(2,4,4-trimethyl-1-pentene)] (PMP) (Fig. 10a)[177]. Experimentally, PMP showed almost no fluorescence both in solution and solid state. In contrast, OMAh exhibited blue and yellow colors in solution and powder under 365 nm irradiation, even for oligomers as short as $M_w \approx 1000$. Theoretical calculations suggest that the short distance between two

neighboring succinic anhydride groups of OMAh rigidifies the oligomeric chain and increases the inter-/intra-chain interactions relative to PMP. Meanwhile, dipolar interactions develop within the oligomer between the positively polarized carbon centers in C=O groups and negatively polarized oxygens of C=O and -O- groups. As a result, the O=C···O=C distances have been predicted to be as short as 2.84 Å. It has been proved that this kind of electrostatic interaction could induce through-space electron delocalization[176]. Notably, the *n*–*π** interactions can also induce a narrow band gap, where *n* electron comes from oxygen and *π* electron from a C=O double bond[178,179]. In this review, both the electrostatic and *n*–*π** interactions are collectively referred to TSC. In PMP, the 2,4,4-trimethyl-1-pentene branches separate the neighboring succinic anhydride groups, thus preventing them from undergoing TSC. The optimized conformation of PMP shows a longer O=C···O=C distance of > 5 Å. The lack of TSC accounts for the lack of luminescence from PMP in both solution and clustered states.

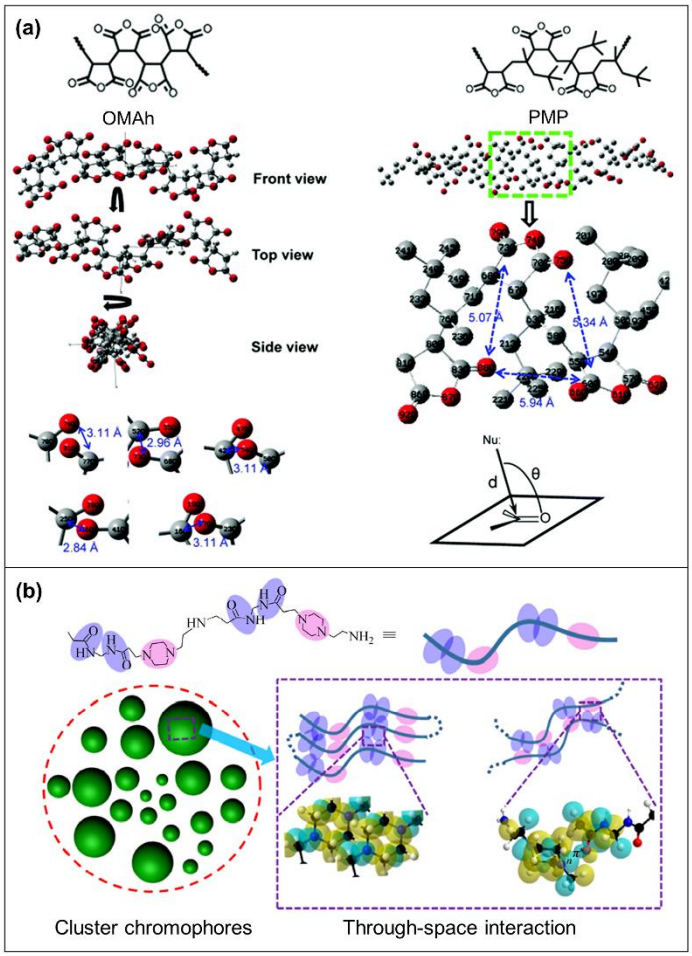

Figure. 10 (a) Optimized conformations of: OMAh (left) and PMP (right) shown from different views. The interaction types of carbonyl groups in OMAh and the proposed model of *n*–*π** interaction are also provided. Reprinted with permission from ref 177. Copyright 2017 Royal Society of Chemistry. (b) Schematic illustration of the cluster chromophores and through-space interaction inside the clusteroluminogens. Reprinted with permission from ref 176. Copyright 2015, Chinese Chemical Society, Institute of Chemistry, Chinese Academy of Sciences and Springer-Verlag Berlin Heidelberg.

The same mechanistic picture was also drawn by Zhu et al[176]. They further used the simulated electron cloud distribution of PAMAM to demonstrate the existence of TSC (Fig. 10b). Meanwhile,

different sizes of clusters that undergo TSC to differing extents and over different conjugation lengths, serving as the source of the excitation-dependent emission effect. Higher generation dendrimers and higher M_w polymers impart larger cluster size. As early as 1970, Roald Hoffmann has studied the interaction of orbitals through space and through bonds[180]. In that work, he pointed out the forbidden nature of ground-state TSC-induced transitions. That is why the TSC species give rise to extremely low-intensity signals in absorption spectra, which are usually undetected. However, the detector sensitivity of fluorescence spectrophotometry is 2-4 orders of magnitude higher than those used for absorption, which makes the TSC signals detectable in excitation spectra. The difference between absorption and excitation spectra may also be attributed to another possible phenomenon: that there is no TSC in the ground state and the light-driven molecular motion induces the formation of TSC in the excited state[41,143]. It seems, therefore, that the presence of TSC can account for all four phenomena presented in Fig. 9.

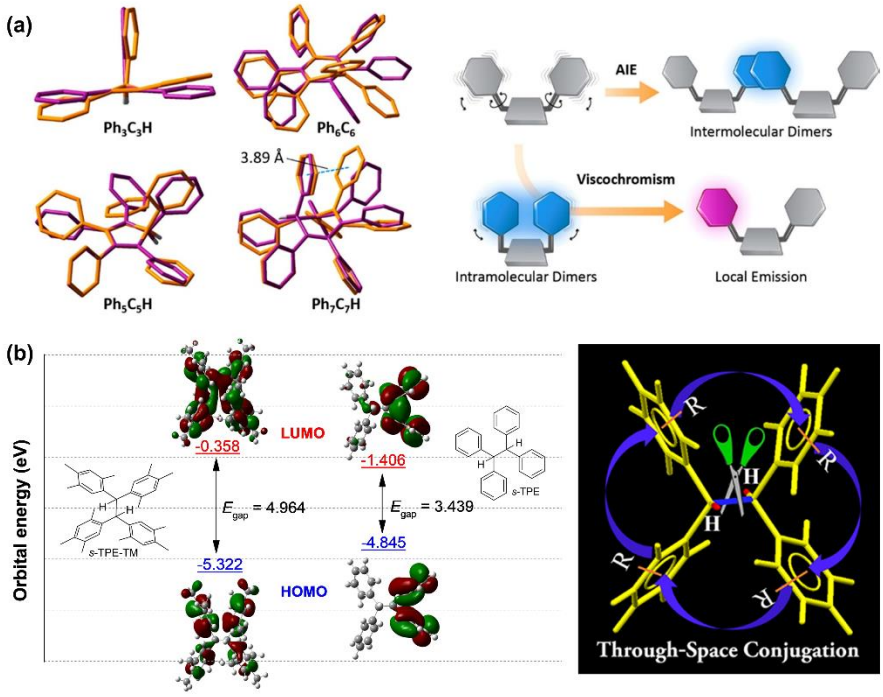

Figure. 11 (a) Left: DFT calculated minimum energy geometries for the S_0 (purple) and S_1 (orange) electronic states of Ph_3C_3H, Ph_5C_5H, Ph_6C_6 and Ph_7C_7H. Right: Schematic representation of the two processes that may lead to the face-to-face aromatic dimer formation. (b) Left: Electron cloud distributions, and energy levels of highest occupied molecular orbitals (HOMO) and lowest unoccupied molecular orbitals (LUMO) in *s*-TPE-TM and *s*-TPE molecules in excited states. Right: Schematic illustration of the through-space conjugation in *s*-TPE. Ref 143 and ref 74. Copyright 2017 American Chemical Society;

Mechanistic studies using monomeric clusteroluminogens have further proved the important role of TSC. As shown in Fig. 11a, geometries calculated for the four phenyl-ring molecular rotors reported by McGonigal et al. suggest that Ph_7C_7H is predisposed to undergoing conformational reorganization to form TSC in the excited state[143]. Only a weak TSC was observed in Ph_5C_5H and there was no such transannular interaction evident in the excited-state geometries of Ph_3C_3H or Ph_6C_6. Meanwhile, McGonigal et al. proposed that, in dilute, high-viscosity solutions, the clusteroluminogens were separated from each other and their molecular motion was restricted, presenting the aromatic rings coming together to create TSC emission. Although molecular motion is also restricted in clustered forms, the close intermolecular packing can lead to

intermolecular TSC, i.e., producing CTE and AIE effects. The same conclusions can also be drawn from evaluating the *s*-TPE-TM and *s*-TPE systems (Fig. 11b)[74]. In *s*-TPE, the HOMO–LUMO energy gap is 5.918 eV in the ground state (GS), which is close to that of benzene. However, its conformation in the excited state (ES) reorders to place two neighboring phenyl rings in a face-to-face intramolecular dimer, decreasing the energy gap to 3.439 eV as a consequence of strong TSC. The additional steric bulk of twelve methyl groups in *s*-TPE-TM partially retard the TSC, so the energy gap decreases by a smaller amount upon excitation, from 5.602 (GS) to 4.964 eV (ES).

3.2 Metal-containing clusteroluminogens

We have introduced the clusterization-triggered fluorescence-to-phosphorescence switching in gold NCs. In 2017, Xu et al. reported the same phenomenon in silver NCs which should emit according to the same mechanism as Au NCs[181]. As shown in Fig. 12a, the Ag complexes with poly[(methyl vinyl ether)-*alt*-(maleic acid)] (PMVEM) ligands fluoresce weakly in aqueous solution. The fluorescence of PMVEM-Ag complexes was attributed to the *n*-π^* interaction-induced TSC in PMVEM, which had little to do with the metal. Meanwhile, the Ag complexes became nonluminescent in solution once the PMVEM ligand was changed to poly(methacrylic acid) (PMAA), because of the steric effect of methyl groups connected to the proximal carbonyl group. With the addition of poor solvent DMSO, NCs were gradually formed and phosphorescence was dominated in the PL spectrum. The authors hypothesized that the poor solvent disrupted the hydrogen bond interactions of PMVEM, resulting in charge shielding of the carboxylate ligands. Then, the carbonyl groups intensively enriched on the surface of Ag core. Further studies reveal that the rigid Ag NCs could boost the π-π^* transition between two neighboring carbonyl groups and result in phosphorescence. However, currently, it is still not clear whether ligand-to-metal (LMCT), metal-to-ligand charge transfer (MLCT) or surface plasmon resonance, contribute to the phosphorescence or not. The Au NCs reported by Xie's group might emit according to the same mechanistic picture as Ag NCs, due to TSC in the glutathione ligands[182-185]. Xie et al. also came up with a method to prepare emissive Au NCs through regulating the thiolate-to-Au ratio (Fig. 12 b)[161]. Conventional Au-thiolate NCs have short Au(I)-thiolate motifs on the surface because of a low thiolate-to-Au ratio, resulting in a large metallic core and thin Au(I)-thiolate surface. By increasing the thiolate-to-Au ratio, the oligomeric Au(I)-thiolate surface to metallic core ratio was also improved. And the size of the metallic core was smaller than the conventional Au-thiolate NCs. Finally, a luminescent Au(0)@Au(I)−thiolate NCs were achieved. Based on the above results, they proposed that the surface of the Au-thiolate NCs played a more important role than the metallic core in terms of the luminescence.

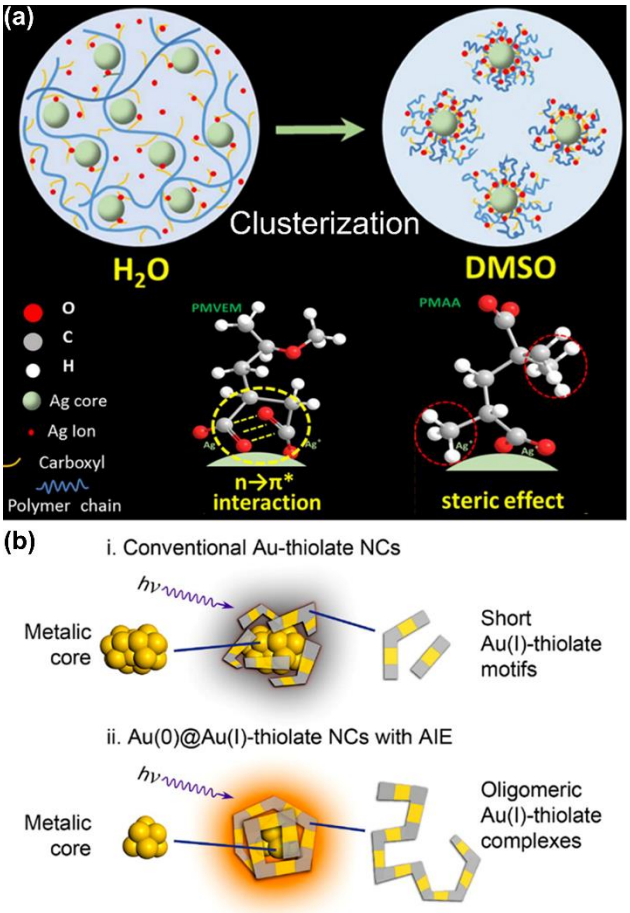

Figure. 12 (a) Schematic illustration of the solvent-induced clusterization of Ag NCs and the different coordination between silver and poly[(methyl vinyl ether)-*alt*-(maleic acid)] (PMVEM) and poly(methacrylic acid) (PMAA) ligands. Ref 181. Copyright 2017, American Chemical Society. (b) Schematic illustration of the structures of (i) conventional Au−thiolate NCs with short Au(I)−thiolate motifs and (ii) luminescent Au NCs. Ref 161. Copyright 2012, American Chemical Society.

According to the above discussion, we present a comprehensive mechanistic picture for clusteroluminescence. Fig. 13a schematically illustrates the process of CTE. From isolated to crosslinked and further to clustered forms, the energy gap (E) of S_n/T_n to S_0 decreases with a red-shifted clusteroluminescence[186-188]. Meanwhile, the increasing size of the clusteroluminogens gradually decreases the energy gap (except for the metal clusters, whose emission blue-shifts with the increase of M_w). It is noteworthy that the smallest units in clusteroluminogens could be n or π electron. We propose that the "chromophore" in clusteroluminogens is built on TSC which involves n-σ^*, n-π^*, π-π^*, hydrogen bonding and other weak interactions[150,189-192]. Inter-/intramolecular TSC will generate a narrow band gap which is the source of clusteroluminescence. Apart from the hydrophobic effect and structural entanglement, inter-/intramolecular electrostatic interactions produced by dipole or transient dipole serve as another driving force for the formation of clusteroluminogens. The transient dipole is generated when the $E^{\delta+}$ and $E^{\delta-}$ moieties possess the same element. Therefore, we divide the mechanistic picture of clusteroluminescence into two parts: i) the formation of clusteroluminogens and ii) TSC-induced clusteroluminescence.

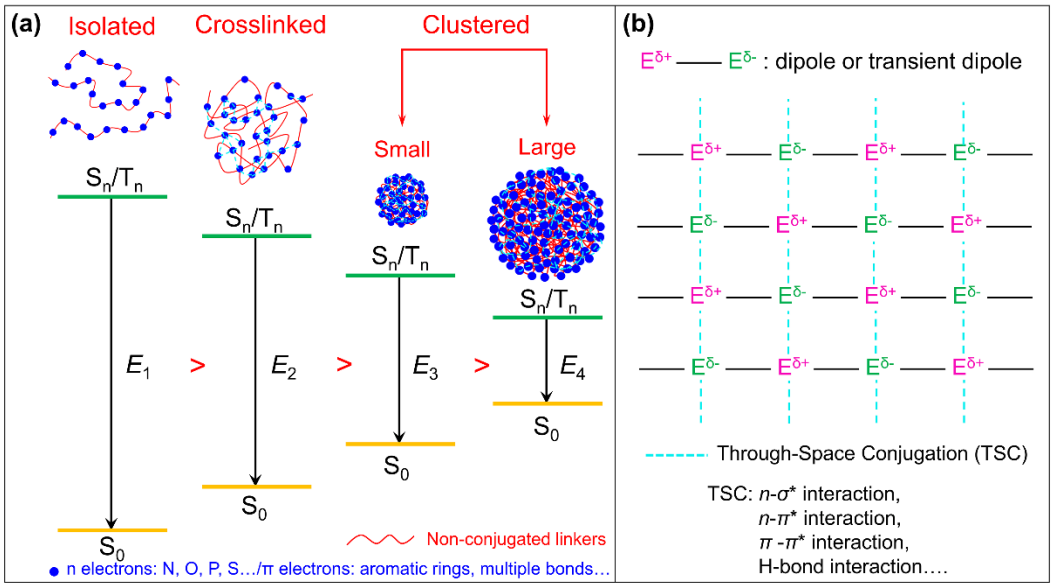

Figure. 13 (a) Schematic illustration of the process of clusters formation accompanied with the clusterization-triggered emission properties. (b) Proposed mechanistic picture for clusteroluminescence.

4. Applications

The mechanistic hypothesis for CTE is consistent with the emission intensity and color from clusteroluminogens being sensitive to their surrounding environments, such as pH, viscosity, degree of dissolution, temperature, etc. In other words, CTE can serve as an indicator of any external stimuli that change the extent of clusterization. In this section, introduce two types of application: i) those involving dynamic responses, i.e., monitoring and visualization and ii) those involving static responses, i.e., applications as sensors and probes.

4.1 Monitoring and visualization

Protein aggregation is associated with many pathological conditions, including Alzheimer's disease, which is caused by the build-up of beta-amyloid fragments within the brain[193-195]. Traditional methods of visualizing protein aggregation depend on covalent attachment of a fluorescent label, which may disrupt the intrinsic folding structure of the protein[196-198]. However, as we have introduced in Section 2.1, some proteins exhibit strong intrinsic fluorescence, not limited to GFP. Is it possible, therefore, to monitor protein aggregation by intrinsic clusteroluminescence? In 2013, Kaminski et al. have successfully tracked protein aggregation through its intrinsic fluorescence[199]. In this work, I59T lysozyme was incubated at 60 °C and pH 5.0 (conditions for aggregation) and its intrinsic fluorescence was imaged by time-correlated single photon counting fluorescence lifetime imaging (TCSPC-FLIM). Fig. 14a shows fluorescence intensity is enhanced and fluorescence lifetime increases slightly with increasing incubation time, which enables the in-situ, real-time and on-site visualization of protein aggregation. As well as biological processes, some abiotic systems can also be monitored by intrinsic fluorescence. We previously discussed (Fig. 4c) the condensation reaction of PIBSA and TETA to form PIBSI bis[115]. The resulting PIBSI bis exhibits stronger clusteroluminescence than PIBSA on account of enhanced TSC within PIBSI bis. As shown in Fig. 14 b, the Φ_F of the reaction system varies with reaction time in the same manner as the degree of functionalization (DF).

Higher DF corresponds to a higher Φ_F. In other words, the clusteroluminescence efficiency can serve as a "meter" to monitor the reaction process. Compared with traditional chromophores, one of the advantages of clusteroluminogens is low toxicity and good biocompatibility. In 2006, Florence et al. used a Gly–$Lys_{63}(NH_2)_{64}$ dendrimer to conduct a cell imaging and uptake study[62]. As shown in Fig. 14c, from 0 to 60 min, gradual entry of the dendrimer into Caco-2 cells is accompanied by the characteristic appearance of green clusteroluminescence. As well as monitoring the uptake process, this method can also be exploited to visualize the cell microstructure.

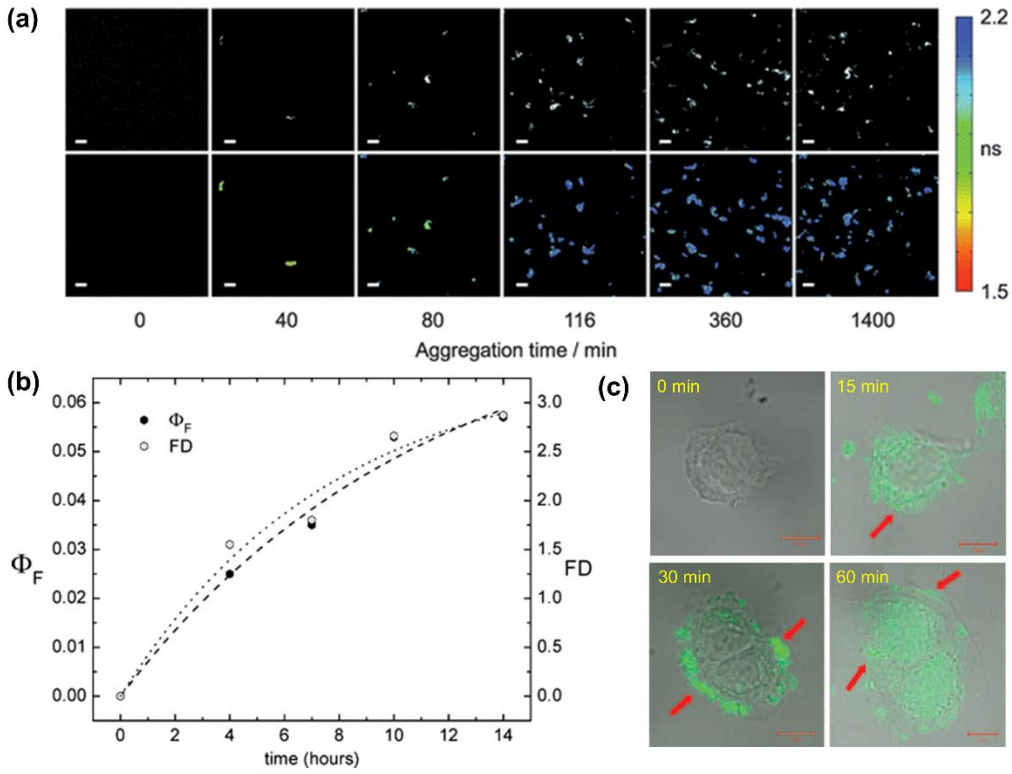

Figure. 14 (a) Change of the fluorescence intensity and lifetime (rows 1 and 2 respectively) of the I59T lysozyme aggregates given for various time-points (0 to 1400 min) during its aggregation process. Scale bars, 20 mm. Reprinted with permission from ref 199. Copyright 2013 Royal Society of Chemistry. (b) Dependence of the fluorescence quantum yield (Φ_F) and the DF of PIBSA derivatives on reaction time; dashed line provide non-linear regression fits of the experimental data. Reprinted with permission from ref 115. Copyright 2008 WILEY‐VCH Verlag GmbH & Co. KGaA, Weinheim. (c) A time-dependent cellular uptake study of the Gly–$Lys_{63}(NH_2)_{64}$ dendrimer (green fluorescent materials) by the Caco-2 cells. Reprinted with permission from ref 62. Copyright 2006 Taylor & Francis.

4.2 Sensors and probes

The luminescence of some clusteroluminogens, such as PAMAM, is sensitive to changes in pH. In 2004, Imae's group noticed that the emission intensity of a G4 NH_2-terminated PAMAM dendrimer gradually increases as the solvent pH decreases from 6 to 2 (Fig. 15a-b)[173], whereas it is almost nonluminescent at pH ≥ 6. The authors hypothesized that, at pH < 6, the protonation of tertiary amine groups populates the dendritic interior with cations, and the resulting charge–charge repulsion makes the structure of PAMAM dendrimer more rigid, which is consistent with CTE. In contrast, the fluorescence of a lower generation dendrimer, G2, is insensitive to change

in pH, which is ascribed to its loose structure. Even when protonated at low pH, the charge–charge repulsion is weak and does not increase the structural rigidity sufficiently to trigger CTE.

It is known that nitro-explosive molecules are typically electron-deficient substrates that can easily bind to electron-rich sites via donor−acceptor interactions, quenching luminescence from electron-rich substrates by electron or charge transfer[200-202]. Clusteroluminogens are good candidates to detect nitro-explosive molecules because of the abundance of *n*- or *π*- electrons in their structures. Recently, Luo et al. have synthesized a hyperbranched PEI−D-glucose polymer nanoparticles (PEI-G PNPs) whose structures contain numerous *n* electrons[203]. Fig. 15c shows that the PL intensity from the PEI-G PNPs gradually decreases with increasing picric acid concentration [PA]. During the process of fluorescence quenching, there are two distinct phases: a steep drop in fluorescence is observed (Fig. 15d) within the [PA] range from 0.05 to 1 μM and slower decrease is observed in the higher [PA] range of 2–70 μM. The different slopes might be caused by different reactivities of the surface and interior of the PNPs. Charge transfer may occur more easily between PA in solution and the *n* electrons at the surface of PNPs, explaining why the slope in the range of 0.05 to 1 μM is steeper than that of 2 to 70 μM.

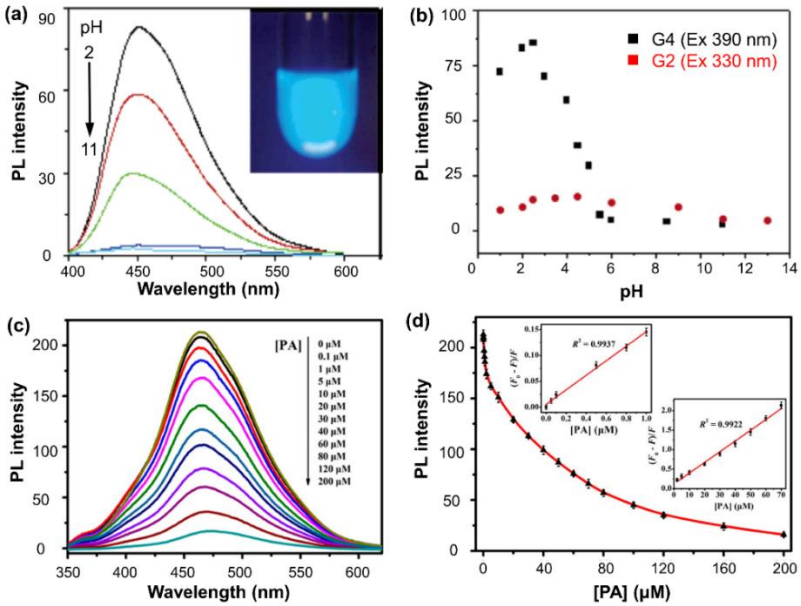

Figure. 15 (a) Fluorescence spectra of a G4 NH_2-terminated PAMAM dendrimer at different pH values, taken under excitation at 390 nm. (b) pH-dependent fluorescence intensity of G2 and G4 NH_2-terminated PAMAM dendrimers, emissions of G2 and G4 were at 410 and 450 nm, respectively. Ref 173. Copyright 2004, American Chemical Society. (c) Fluorescence spectra of poly(ethylenimine)-D-glucose (PEI-G) after the addition of various concentrations of picric acid (PA), as indicated on the frame. Excitation: 345 nm. (d) Plot of the maximum fluorescence intensity of hyperbranched PEI-G versus [PA]. Inset: Linear relationships of $(F_0 - F)/F$ vs. [PA] from 0 to 1 μM and from 2 to 70 μM, where F_0 and F denote the maximum fluorescence intensity of PEI-G PNPs before and after addition of PA, respectively. Ref 203. Copyright 2016, American Chemical Society.

5. Summary and perspective

In this review, we have summarized a recently recognized class of materials – clusteroluminogens which exhibit clusterization-triggered emission (CTE). In contrast to the conventional chromophores, the systematic investigation of clusteroluminogens has a rather short history,

although the related optical phenomenon has been observed in natural products hundreds of years ago. We argue that clusteroluminescence operates by different photophysical mechanism from the luminescence of traditional *π*-conjugated systems. Herein, three types of clusteroluminogens have been introduced, namely polymers, small molecules, and metal–organic clusters. Both synthetic and natural polymers have been found that undergo CTE, and small-molecule clusteroluminogens are known both with and without aromatic rings in their structures. Through-space conjugation (TSC), arising from *n*–*σ**, *n*–*π**, and *π*–*π** orbital overlap, as well as hydrogen bonding and other weak interactions, has been proposed as the key structural feature for the organic clusteroluminescence. The ligands of clusterluminescent metal clusters are synthetic polymer clusteroluminogens in most cases, serving as part of chromophores for the luminescence in clustered states. Additionally, MLCT, LMCT, and surface plasmon resonance, etc. may also play crucial role in the clusteroluminescence of NCs, deserving in-depth investigation.

To summarize, by analyzing the experimental data presented in this review, we put forward the following six characteristic features of CTE. It is possible that they may not be applicable to all the clusteroluminogens simultaneously.

I) Clusteroluminogens are based upon non-conjugated molecular motifs, where *n* or *π* electron-based groups are separated by nonconjugated linkers.
II) In the isolated states, only the electron transition belonging to *n* or *π* electron-based groups can be detected in the PL spectra of clusteroluminogens. However, an intrinsic luminescence appears at longer wavelengths upon clustering of these molecules, which is termed as the clusteroluminescence.
III) The excitation spectra of clusteroluminogens appear red-shifted in comparison with their absorption spectra. In other words, these molecules are excited by light whose wavelength is out of the range of strong absorption peaks.
IV) Clusteroluminogens show excitation-dependent luminescence properties, where excitation at longer wavelength results in a red-shifted emission.
V) Clusteroluminogens show size-dependent emission properties. The conception of “size” is related to different generations of dendrimers, molecular weights of the polymers, diameter of the nanoparticles, etc. Generally, the increase of size would shift PL spectra to the red, and the emission intensity will be enhanced.
VI) Clusteroluminogens, especially polymer systems, are capable to phosphoresce, and some of them show room-temperature phosphorescence.

One can envisage that CTE will be applicable in several areas, such as those discussed in this Review–the process monitoring of cellular uptake and reactions, structure visualization, sensing and as probes. The CTE effect can be exploited in circumstances that change the conformations of clusteroluminogens, i.e., by exposing them to changes in temperature, pH, solubility, viscosity, mechanical force, irradiation, ionic strength, etc. Changes in the observed clusteroluminescence then serve as an indicator to visualize and monitor dynamic processes and their static structures. Compared to existing types of probe molecules, clusteroluminogens may come into their own due to their low toxicities and good biocompatibilities, which are advantageous in biological applications. Besides applications, mechanistic studies into the CTE effect offer the prospect of breakthroughs in theory. Currently, photophysical models for traditional *π*-conjugated systems are not directly applicable to clusteroluminogens. We believe that recognizing TSC as a prerequisite for clusteroluminescence is an only prelude to further advances.

Acknowledgments

We are grateful for financial support from the National Science Foundation of China (21788102), the Research Grants Council of Hong Kong (16308016, CityU11305617, C6009-17G and A-HKUST 605/16), the University Grants Committee of Hong Kong (AoE/P-03/08 and AoE/P-02/12), the Innovation and Technology Commission of Hong Kong (ITC-CNERC14SC01 and ITS/254/17) and the Science and Technology Plan of Shenzhen (JCYJ20160229205601482, JCYJ20170818104224667 and JCY20170818113602462).

References

[1] Z. Zhao et al., Soft. Matter. 9 (2013) 4564-4579.
[2] F.Y. Song et al., Adv. Funct. Mater. 28 (2018) 1800051.
[3] Y.C. Li et al., Mater. Today. 20 (2017) 258-266.
[4] F. Zhao,D. Ma, Mater. Chem. Front., 1 (2017) 1933-1950.
[5] W.H. Xu et al., Chem. Sci. 10 (2019) 3494-3501.
[6] X.Y. Shen et al., Chem. Comm. 50 (2014) 8747-8750.
[7] L.Z. Li et al., Chem. Comm. 51 (2015) 4830-4833.
[8] S.J. Liu et al., J. Am. Chem. Soc.141 (2019) 5359-5368.
[9] C. Zhu et al., ACS Appl. Bio Mater. 1 (2018) 1768-1786.
[10] H. Zhang et al., Mater. Chem. Front. 3(2019) 1143-1150.
[11] M. Chen et al., ACS Appl. Mater. Interfaces 10 (2018) 12181-12188.
[12] J.B. Birks et al., Proc. Royal Soc. A 283 (1965) 83-99.
[13] T. Förster,K. Kasper, Z. Phys. Chem. 1 (1954) 275−277.
[14] J. Luo et al., Chem. Comm. (2001) 1740-1741.
[15] Y.N. Hong et al., Chem. Soc. Rev. 40 (2011) 5361-5388.
[16] J. Mei et al., Chem. Rev. 115 (2015) 11718-11940.
[17] Z.Y. Wang et al., J. Phys. Chem. B 122 (2018) 2165-2176.
[18] J. Zhang et al., ACS Nano 13 (2019) 3618-3628.
[19] H.K. Zhang et al., J. Mater. Chem. C 3 (2015) 5162-5166.
[20] W.Z. Yuan et al., Adv. Mater. 22 (2010) 2159-2163.
[21] X.Z. Yan et al., Nat. Chem. 7 (2015) 342-348.
[22] X.Z. Yan et al., J. Am. Chem. Soc.137 (2015) 15276-15286.
[23] H.J. Liu et al., Angew. Chem. Int. Ed. 57 (2018) 9290-9294.
[24] S. Xie et al., Angew. Chem. Int. Ed. 57 (2018) 5750-5753.
[25] R.T.K. Kwok et al., Chem. Soc. Rev. 44 (2015) 4228-4238.
[26] K. Li,B. Liu, Chem. Soc. Rev. 43 (2014) 6570-6597.
[27] E.G. Zhao et al., Adv. Mater. 27 (2015) 4931-4937.
[28] Y.C. Chen et al., Angew. Chem. Int. Ed. 57 (2018) 5011-5015.
[29] J. Mei et al., Adv. Mater. 26 (2014) 5429-5479.
[30] L. Wang et al., Sci. China Chem. 59 (2016) 1609-1615.
[31] S.J. Liu et al., Angew. Chem. Int. Ed. 57 (2018) 6274-6278.
[32] Y.H. Cheng et al., Mater. Horiz. 6 (2019) 405-411.
[33] H. Zhang et al., "Aggregation and chirality," Proc. SPIE, Liquid Crystals XXII (2018) 107350H.
[34] P. Alam et al., Angew. Chem. Int. Ed. 58 (2019) 4536-4540.
[35] Z. Zhao et al., Nat. Commun. 10 (2019) 768.
[36] Z.Y. Wang et al., ACS Appl. Mater. Interfaces11 (2019) 17306-17312.
[37] J. Qian,B.Z. Tang, Chem 3 (2017) 56-91.
[38] J. Qi et al., Adv. Healthc. Mater. 7 (2018) 1800477.
[39] Y.Y. Gong et al., Sci. China Chem. 56 (2013) 1178-1182.

[40] S. Zhu et al., Chem. Commun. 48 (2012) 10889-10891.
[41] H. Zhang et al., ChemRxiv (2019) 10.26434/chemrxiv.8280464.
[42] J.J. Yan et al., Adv. Mater. 24 (2012) 5617-5624.
[43] X. Chen et al., Macromolecules 51 (2018) 9035-9042.
[44] F. Bacon. The Advancement of Learning, London, 1605.
[45] P. Wang et al., ACS Appl. Mater. Interfaces 11 (2019) 19301-19307.
[46] L.L. Du et al., Chinese J. Polym. Sci. 37 (2019) 409-415.
[47] W.Z. Yuan, Y. Zhang, J. Polym. Sci. A 55 (2017) 560-574.
[48] J.I. Zink et al., J. Phys. Chem. 80 (1976) 248-249.
[49] M. Li et al., Front. Chem. 7 (2019) 447.
[50] C.M. Xing et al., Polym. Mater. Sci. Eng. 96 (2007) 418-419.
[51] W.Z. Yuan,Y.M. Zhang, J. Polym. Sci. A 55 (2017) 560-574.
[52] V. Bekiari, P. Lianos, Langmuir 14 (1998) 3459-3461.
[53] V. Bekiari et al., Chem. Mater. 12 (2000) 3095-3099.
[54] L.D. Carlos et al., Adv. Mater. 19 (2007) 341-348.
[55] H. Lu et al., Phys. Chem. Chem. Phys. 17 (2015) 26783-26789.
[56] S. Niu et al., Macromol. Chem. Phys. 217 (2016) 1185-1190.
[57] H. Lu et al., Macromolecules 48 (2015) 476-482.
[58] C.L. Larson, S.A. Tucker, Appl. Spectrosc. 55 (2001) 679-683.
[59] O. Varnavski et al., J. Chem. Phys. 114 (2001) 1962-1965.
[60] W.I. Lee et al., J. Am. Chem. Soc.126 (2004) 8358-8359.
[61] X.Y. Liu et al., Langmuir. 31 (2015) 4386-4393.
[62] K.T. Al-Jamal et al., J. Drug Target. 14 (2006) 405-412.
[63] P. Marek et al., Chembiochem 9 (2008) 1372-1374.
[64] K.K. Turoverov, I.M. Kuznetsova, J. Fluoresc. 13 (2003) 41-57.
[65] Z.K. He et al., ACS Omega 3 (2018) 3267-3277.
[66] H. Wang et al., Mater. Today 18 (2015) 365-377.
[67] Y. Zhang et al., Polym. Chem. 9 (2018) 558-564.
[68] D. Schilter, Nat. Rev. Chem. 1 (2017) 0097.
[69] D.A. Tomalia et al., Prog. Polym. Sci. 90 (2019) 35-117.
[70] M. Studzian et al., J. Phys. Chem. C (2019) DOI: 10.1021/acs.jpcc.9b02725 .
[71] M. Konopka et al., J Nanopart, Res, 20 (2018) 220.
[72] M. Konopka et al., Polymers 10 (2018) 540.
[73] R. Ye et al., Polym. Chem. 8 (2017) 1722-1727.
[74] H.K. Zhang et al., J. Am. Chem. Soc.139 (2017) 16264-16272.
[75] C. Shang et al., J. Mater. Chem. C 5 (2017) 8082-8090.
[76] B. van Dam et al., Small 13 (2017).
[77] C. Li et al., Sensor. Actuat. B-Chem. 263 (2018) 1-9.
[78] Z. Zhao et al., Polym. Chem. (2019).
[79] Y. Li et al., Spectrosc. Spect. Anal. 31 (2011) 422-426.
[80] L. Deng et al., Nano Res. 8 (2015) 2810-2821.
[81] Q. Zhou et al., Mater. Chem. Front., 3 (2019) 257-264.
[82] T. Zhang et al., Chem. Asian J. 14 (2019) 884-889.
[83] P.F. Wei et al., Chem. Mater. 31 (2019) 1092-1100.
[84] O. Shimomura et al., J. Cell. Physiol. 59 (1962) 223-239.
[85] P.S. Weiss, ACS Nano 2 (2008) 1977-1977.
[86] M.J. Jiang et al., J. Mater. Chem. C 5 (2017) 7191-7199.
[87] D.P. Barondeau et al., Proc. Natl. Acad. Sci. U.S.A100 (2003) 12111-12116.
[88] J. Galban et al., Luminescence 16 (2001) 199-210.
[89] A. Shukla et al., Arch. Biochem. Biophys 428 (2004) 144-153.
[90] Z. Xu et al., J. Bacteriol. 185 (2003) 4038-4049.
[91] Z.Y. Zhang et al., Adv. Phys. X 3 (2018) 1428915 .

[92] L.L. Del Mercato et al., Proc. Natl. Acad. Sci. U.S.A 104 (2007) 18019-18024.
[93] X. Dou et al., Biomacromolecules 19 (2018) 2014-2022.
[94] P. Kesharwani et al., Mater. Today 18 (2015) 565-572.
[95] M.S. Diallo et al., Env. Sci. Tech. 33 (1999) 820-824.
[96] D.A. Tomalia et al., Angew. Chem. Int. Ed. 29 (1990) 138-175.
[97] D.A. Tomalia et al., Polym. J. 17 (1985) 117-132.
[98] G. Caminati et al., J. Am. Chem. Soc.112 (1990) 8515-8522.
[99] K. Tamano, T. Imae, J. Nanosci. Nanotechnol. 8 (2008) 4329-4334.
[100] L. Crespo et al., Chem. Rev. 105 (2005) 1663-1681.
[101] G. Jayamurugan et al., Org. Lett. 10 (2008) 9-12.
[102] T. Huang et al., Acta Chim. Sinica 71 (2013) 979.
[103] W.H. Luo et al., J. Colloid Interface Sci. 509 (2018) 327-333.
[104] D.C. Wu et al., Macromolecules 38 (2005) 9906-9909.
[105] S.Y. Lin et al., Chem. Eur. J. 17 (2011) 7158-7161.
[106] L. Pastor-Pérez et al., Macromol. Rapid. Comm. 28 (2007) 1404-1409.
[107] X. Chen et al., Mol. Syst. Des. Eng. 3 (2018) 364-375.
[108] Q. Zhou et al., Small 12 (2016) 6586-6592.
[109] Y. Joo et al., Science 359 (2018) 1391-1394.
[110] Y. Wang et al., Macromol. Rapid. Commun. 39 (2018) 1800528.
[111] Y. Du et al., Polym. J. (2019) DOI: 10.1038/s41428-019-0208-1.
[112] C.M. Xing, W.T. Yang, Macromol. Rapid. Commun. 25 (2004) 1568-1574.
[113] M. Bosma et al., Polymer 29 (1988) 1694-1698.
[114] V. Sunel et al., Mater. Plast. 45 (2008) 149-153.
[115] A. Pucci et al., Macromol. Chem. Phys. 209 (2008) 900-906.
[116] Z. Guo et al., Macromol. Rapid. Commun. 38 (2017) 1700099.
[117] C.X. Hu et al., Macromol. Rapid. Commun. 39 (2018) 180003.
[118] Y. Ru et al., Polym. Chem. 7 (2016) 6250-6256.
[119] W.J. Zhao et al., Nat. Commun. 10 (2019) 1595.
[120] J. Wang et al., J. Am. Chem. Soc.134 (2012) 9956-9966.
[121] H.Q. Peng et al., ACS Nano 13 (2019) 839-846.
[122] Z.Y. Yang et al., J. Mater. Chem. C 4 (2016) 99-107.
[123] X. Shang et al., Sci. Rep. 7 (2017) 5508.
[124] Y. Shi et al., Sci. China Chem. 60 (2017) 635-641.
[125] Y. Hu et al., ACS Appl. Polym. Mater. 1 (2019) 221-229.
[126] S.S. Yanari et al., Nature 200 (1963) 242-244.
[127] F. Hirayama, J. Chem. Phys. 42 (1965) 3163-3171.
[128] Y.Y. Zhang et al., J. Mater. Chem. C 4 (2016) 9316-9324.
[129] A.G. Martinez et al., J. Am. Chem. Soc.120 (1998) 673-679.
[130] L. Chen et al., Angew. Chem. Int. Ed. 54 (2015) 4231-4235.
[131] P.C. Shen et al., J. Phys. Chem. Lett. 10 (2019) 2648-2656.
[132] P.C. Shen et al., Chin. Chem. Lett. 27 (2016) 1115-1123.
[133] Q. Zhu et al., Chem. Sci. 6 (2015) 4690-4697.
[134] T. Han et al., J. Am. Chem. Soc.140 (2018) 5588-5598.
[135] L. Viglianti et al., Chem. Sci. 8 (2017) 2629-2639.
[136] M.D. Esrafili, M. Vakili, J Mol. Model. 20 (2014) 2291.
[137] I.S. Antonijevic et al., Cryst. Growth Des. 16 (2016) 632-639.
[138] Y.J. Cai et al., Chem. Sci. 9 (2018) 4662-4670.
[139] Z. Qiu et al., Macromolecules 49 (2016) 8888-8898.
[140] Y.J. Liu et al., Macromolecules 48 (2015) 8098-8107.
[141] Y.J. Gao et al., J. Phys. Chem. . A 121 (2017) 2572-2579.
[142] A. Prlj et al., Phys. Chem. Chem. Phys. : PCCP 18 (2016) 11606-11609.
[143] J. Sturala et al., J. Am. Chem. Soc.139 (2017) 17882-17889.

[144] S.J. Zhen et al., Nano Lett. 18 (2018) 4200-4205.
[145] J. Li et al., CCS Chem. 1 (2019) 181-196.
[146] X. Chen et al., Sci. China Chem. 61 (2017) 351-359.
[147] Q. Zhang et al., J. Mater. Chem. C 5 (2017) 3699-3705.
[148] J. Yan et al., Polym. Chem. 6 (2015) 6133-6139.
[149] A.M. Halpern, Chem. Phys. Lett. 6 (1970) 296-298.
[150] A.M. Halpern et al., J. Chem. Phys. 49 (1968) 1348-1357.
[151] H. Basch et al., J. Chem. Phys. 47 (1967) 1201-1210.
[152] R. Colle et al., Theor. Chim. Acta. 44 (1977) 1-7.
[153] C.C. Chu, T. Imae, Macromol. Rapid. Commun. 30 (2009) 89-93.
[154] H. Zhang, Aggregation-Induced Emission: Mechanistic Study, Clusteroluminescence and Kinetic Resolution, PhD Thesis, Hong Kong University of Science and Technology, 2018.
[155] L. Sobczyk et al., Chem. Rev. 105 (2005) 3513-3560.
[156] L. Rincon et al., J. Chem. Phys. 114 (2001) 5552-5561.
[157] L. Wang et al., Proc. Natl. Acad. Sci. U.S.A 111 (2014) 18454-18459.
[158] B. Wang et al., Phys. Chem. Chem. Phys. 17 (2015) 2987-2990.
[159] V.I. Lobyshev et al., J. Mol. Liq. 82 (1999) 73-81.
[160] W.Z. Yuan et al., Angew. Chem. Int. Ed. (2019) DOI: 10.1002/anie.201906226.
[161] Z. Luo et al., J. Am. Chem. Soc.134 (2012) 16662-16670.
[162] M. Sugiuchi et al., J. Am. Chem. Soc.139 (2017) 17731-17734.
[163] X.H. Wu et al., Adv. Sci. 6 (2019) 1801304.
[164] R.W. Huang et al., Nat. Chem. 9 (2017) 689-697.
[165] X. Jia et al., Small 9 (2013) 3873-3879.
[166] X. Kang, M. Zhu, Coord. Chem. Rev. 394 (2019) 1-38.
[167] H. Liu et al., Analyst (2019) DOI: 10.1039/c9an00667b.
[168] Z.G. Wang et al., Adv. Funct. Mater. 28 (2018) 1802848.
[169] X. Yan et al., J. Am. Chem. Soc.141 (2019) 9673-9679.
[170] Z. Zhou et al., J. Am. Chem. Soc.141 (2019) 5535-5543.
[171] L.N. Xu et al., J. Am. Chem. Soc.140 (2018) 16920-16924.
[172] Z. Wang et al., Adv. Sci. 3 (2016) 1600182.
[173] D.J. Wang, T. Imae, J. Am. Chem. Soc.126 (2004) 13204-13205.
[174] J. Liu et al., Macromolecules 43 (2010) 4921-4936.
[175] K.M. Lee et al., Nat. Commun. 4 (2013) 1544.
[176] R.B. Wang et al., Chinese J. Polym. Sci. 33 (2015) 680-687.
[177] X. Zhou et al., J. Mater. Chem. C 5 (2017) 4775-4779.
[178] R.W. Newberry, R.T. Raines, ACS Chem. Biol. 9 (2014) 880-883.
[179] D.J. Schmucker et al., J. Phys. Chem. A 123 (2019) 2537-2543.
[180] R. Hoffmann, Acc. Chem. Res. 4 (1971) 1-9.
[181] T. Yang et al., J. Phys. Chem. lett. 8 (2017) 3980-3985.
[182] X. Yuan et al., Nano Res. 7 (2013) 301-307.
[183] K. Zheng et al., Chem. Comm. 51 (2015) 15165-15168.
[184] Z. Wu et al., Angew. Chem. Int. Ed. 58 (2019) 8139-8144.
[185] N. Goswami et al., J. Phys. Chem. lett. 7 (2016) 962-975.
[186] H. Qian et al., Nat. Chem. 9 (2017) 83-87.
[187] J.J. Guo et al., Adv. Sci. 6 (2019) 1801629.
[188] Z.K. He et al., Nat Commun 8 (2017) 416.
[189] B.H. Jhun et al., J. Phys. Chem. C 121 (2017) 11907-11914.
[190] A. Ohrn,G. Karlstrom, J. Phys. Chem. A 110 (2006) 1934-1942.
[191] N.J. Turro et al., Modern molecular photochemistry of organic molecules. University Science Books: Sausalito, Calif., 2010.
[192] I.V. Alabugin, Stereoelectronic effects: a bridge between structure and reactivity. John Wiley & Sons, Ltd. Chichester, 2016.

[193] https://www.eurekalert.org/pub_releases/2019-01/hkuo-hsd011119.php
[194] H.K. Zhang et al., Nat. Commun. 9 (2018) 4961.
[195] G.B. Irvine et al., Mol. Med. 14 (2008) 451-464.
[196] Y.N. Hong et al., Anal. Chem. 82 (2010) 7035-7043.
[197] Y.N. Hong et al., J. Am. Chem. Soc.134 (2012) 1680-1689.
[198] M.Z. Chen et al., Nat. Commun. 8 (2017) 14548.
[199] F.T. Chan et al., Analyst 138 (2013) 2156-2162.
[200] W.Y. Dong et al., Polym. Chem. 5 (2014) 4048-4053.
[201] H. Zhou et al., Polym. Chem. (2019) DOI: 10.1039/C9PY00322C.
[202] Z.W. Chu et al., Sensors 18 (2018) 1565.
[203] S.G. Liu et al., ACS Appl. Mater. Interfaces 8 (2016) 21700-21709.